



**HAL**  
open science

# Unraveling the Roles of Saltation Bombardment and Atmospheric Instability on Magnitude and Size Distribution of Dust Emission Fluxes: Lessons From the JADE and WIND-O-V Experiments

S. C. Alfaro, C. Bouet, B. Khalfallah, Y. Shao, M. Ishizuka, M. Labiadh, B. Marticorena, B. Laurent, J. L. Rajot

## ► To cite this version:

S. C. Alfaro, C. Bouet, B. Khalfallah, Y. Shao, M. Ishizuka, et al.. Unraveling the Roles of Saltation Bombardment and Atmospheric Instability on Magnitude and Size Distribution of Dust Emission Fluxes: Lessons From the JADE and WIND-O-V Experiments. *Journal of Geophysical Research: Atmospheres*, 2022, 127 (12), pp.e2021JD035983. 10.1029/2021JD035983 . insu-03749603

**HAL Id: insu-03749603**

**<https://insu.hal.science/insu-03749603>**

Submitted on 7 Apr 2023

**HAL** is a multi-disciplinary open access archive for the deposit and dissemination of scientific research documents, whether they are published or not. The documents may come from teaching and research institutions in France or abroad, or from public or private research centers.

L'archive ouverte pluridisciplinaire **HAL**, est destinée au dépôt et à la diffusion de documents scientifiques de niveau recherche, publiés ou non, émanant des établissements d'enseignement et de recherche français ou étrangers, des laboratoires publics ou privés.

Copyright

## RESEARCH ARTICLE

10.1029/2021JD035983

### Key Points:

- During erosion events, vertical dust flux is not linearly proportional to saltation flux
- The size of emitted dust is controlled by the kinetic energy of the saltating sand grains
- The vertical dust flux is enriched in fine particles during intense events and in unstable conditions

### Supporting Information:

Supporting Information may be found in the online version of this article.

### Correspondence to:

C. Bouet,  
[christel.bouet@ird.fr](mailto:christel.bouet@ird.fr)

### Citation:

Alfaro, S. C., Bouet, C., Khalfallah, B., Shao, Y., Ishizuka, M., Labiadh, M., et al. (2022). Unraveling the roles of saltation bombardment and atmospheric instability on magnitude and size distribution of dust emission fluxes: Lessons from the JADE and WIND-O-V experiments. *Journal of Geophysical Research: Atmospheres*, 127, e2021JD035983. <https://doi.org/10.1029/2021JD035983>

Received 5 OCT 2021

Accepted 9 JUN 2022

# Unraveling the Roles of Saltation Bombardment and Atmospheric Instability on Magnitude and Size Distribution of Dust Emission Fluxes: Lessons From the JADE and WIND-O-V Experiments

S. C. Alfaro<sup>1</sup> , C. Bouet<sup>2,3</sup> , B. Khalfallah<sup>1</sup> , Y. Shao<sup>4</sup> , M. Ishizuka<sup>5</sup> , M. Labiadh<sup>6</sup> , B. Marticorena<sup>1</sup> , B. Laurent<sup>3</sup> , and J. L. Rajot<sup>2,3</sup> 

<sup>1</sup>Univ Paris Est Creteil and Université Paris Cité, CNRS, LISA, Créteil, France, <sup>2</sup>Univ Paris Est Creteil - Sorbonne Université - Université Paris Cité - IRD - CNRS - INRAE, iEES Paris, Bondy, France, <sup>3</sup>Université Paris Cité and Univ Paris Est Creteil, CNRS, LISA, Paris, France, <sup>4</sup>Institute for Geophysics and Meteorology, University of Cologne, Cologne, Germany, <sup>5</sup>Faculty of Engineering and Design, Kagawa University, Takamatsu, Japan, <sup>6</sup>IRA (Institut des Régions Arides) de Médénine, El Fjé, Medenine, Tunisia

**Abstract** The size distribution of the vertical flux of dust freshly emitted from a wind-eroded surface was recently shown to depend on the thermal stratification of the surface boundary layer (SBL). These new results question the way dust emission is currently represented in the dust models and emphasize the need to identify the factors controlling the intensity and size-resolved dust flux at emission. In this study, we re-analyze the data of two major campaigns (JADE and WIND-O-V) performed on unvegetated plots and during which the characteristics of the (a) surface of the eroding fields, (b) aerodynamic conditions (wind speed, stability of the SBL), (c) saltation flux (intensity and size distribution), and (d) vertical dust flux (intensity and size distribution) determined by the gradient method were carefully documented. The magnitude and size distribution of the vertical dust flux are found to be deeply intertwined and to be controlled in the first place by the kinetic energy of the saltating sand grains, and to a lesser extent by the size-dependent uplift of the sandblasted particles. In unstable conditions coarser sand grains are mobilized, which increases the kinetic energy of the saltation flux and leads to the production of finer particles by sandblasting. Conversely, the uplift of supermicron particles is facilitated by the increase of the wind friction velocity, which results in an enrichment of the vertical dust flux in the coarsest particles at large wind speeds. The implications of these new findings are particularly important for the modeling of the dust emission/transport/deposition cycle.

## 1. Introduction

Each year, wind erosion of arid and semi-arid soils releases between 1,000 and 4,000 Tg of mineral dust into the atmosphere (Boucher et al., 2013). The environmental impacts of these particles are well recognized (for a review see Middleton, 2017), but their magnitude is still poorly constrained because of the uncertainties on the magnitude and Particle Size Distribution (dust-PSD) of the dust flux at emission (e.g., Evan et al., 2014; Zhao et al., 2022). Indeed, the size distribution controls the residence time and long range transport of the particles, their interactions with solar and terrestrial radiations, and their reactivity with the other gaseous and particulate components of the atmosphere (e.g., Mahowald et al., 2014).

Wind-tunnel simulations of the two main aeolian processes (saltation and sandblasting) whose combination leads to the production of dust smaller than 20  $\mu\text{m}$  in diameter ( $\text{PM}_{20}$ ) were performed to document the influence of aerodynamic conditions on the dust-PSD (Alfaro et al., 1997, 1998; Shao et al., 1993; Wang et al., 2021). These authors showed that the proportion of very fine particles increased with wind speed. Based either on these observations (Alfaro & Gomes, 2001) or on more theoretical considerations (Shao, 2001), two physically-based dust production models were developed. The gist of the Alfaro and Gomes (2001) model is that the kinetic energy of the soil aggregates moving close to the soil increases with wind speed and that finer and finer particles are released as their impacts on the ground become more energetic. In the Shao (2001) model, the dust flux is composed of particles resulting from (a) the disintegration of the saltating particles and (b) the ejection of soil particles by saltation bombardment. The dust-PSD in this model is similar to that of the parent soil but evolves gradually from minimally dispersed during the weak erosion events to fully dispersed, and is thus enriched in

finer particles as the wind erosion becomes stronger. Thus, though differing in their formulations, the models proposed by Alfaro and Gomes (2001) and by Shao (2001) concur on the point that the dust-PSD should shift toward finer sizes as the wind speed increases.

A third theory of the sandblasting was proposed by Kok (2011b). Basically, this “brittle fragmentation theory” assumes that (a) microfractures preexist in the saltating grains, (b) their breakage resulting from the impacts releases fine particles, and (c) the mean impact speed of the saltators are independent of wind speed when saltation has reached equilibrium. A consequence of these assumptions is that the dust PSD should be independent of  $u_*$  (Kok, 2011a) when nothing opposes the development of saltation, which is to say over surfaces with sufficiently long fetch, unlimited supply of loose erodible material, and deprived of vegetation.

To date, a number of field campaigns have been performed to characterize in natural conditions the influence of wind speed on the dust emission flux and its size distribution. Most of them were performed over “near-ideal” surfaces (i.e., unvegetated and non supply-limited sandy surfaces), but others were also carried out in presence of sparse vegetation and crusts to document their impact on the dust-PSD (Webb et al., 2021). Among the experiments of the first category, one took place in Niger in the framework of the African Monsoon Multidisciplinary Analysis (AMMA) intensive observation periods (Sow et al., 2009) and another one in Australia during the Japanese Australian Dust Experiment (JADE) (Ishizuka et al., 2008; Shao et al., 2011). Sow et al. (2009) showed that the dust-PSD was finer during the most energetic convective erosion event (CE4) than during the more moderate events of the monsoon type (ME1 and ME4), which tended to support globally the model of Alfaro and Gomes (2001) and that of Shao (2001). However, because the evolution of the dust-PSD during each event did not clearly follow the variations of wind speed, no definitive conclusion regarding the influence of  $u_*$  could be drawn from the analysis of these observations.

More recently, a third intensive experiment was carried out in south Tunisia in the framework of the WIND-O-V (WIND erOsion in presence of sparse Vegetation) project (Dupont et al., 2018, 2019). For the first time, the measurements showed that the PSD of the vertical dust flux measured between 2 and 4 m above the eroding surface was sensitive to the thermal stratification of the Surface Boundary Layer (SBL) (Khalfallah et al., 2020), but again no clear dependence to wind speed was found. The authors interpreted the observed variations of the vertical dust flux size distribution as resulting from a size-dependent efficiency of the vertical uplift of the dust particles released from the surface.

The publication of the latter results led Shao et al. (2020) to re-analyze the data of the 12 events of the JADE experiment among which three were singled out as case studies because they had contrasted thermal stratification (events #10 and #11) or different surface state (event #12). They concluded that their re-analysis confirmed the dependency of the dust-PSD not only to thermal instability but also to wind speed. The explanation proposed by these authors for the dependency of the dust-PSD on the stability conditions was that in unstable conditions the wind speed was more variable than in neutral ones. Therefore, at similar average  $u_*$ , it peaked at larger values in unstable surface layers and communicated more kinetic energy to the saltating soil aggregates, which resulted in the emission of finer dust. Noteworthy, the interpretations of Khalfallah et al. (2020) and Shao et al. (2020) are not mutually exclusive and the relative enrichment of the vertical flux in fine particles observed in thermally unstable conditions could be explained by the combination of a more energetic saltation bombardment and a size-selective vertical uplift of the particles produced by sandblasting. In any case, these new results are expected to complicate the representation of the characteristics of the dust-emission flux in the models and it is important to understand better the factors controlling the emission of mineral dust by wind erosion.

Although direct entrainment of fine soil material by wind is possible (Klose & Shao, 2012), especially during convective conditions, saltation is by far a more efficient wind-erosion process (Shao et al., 2011). This is the bombardment of the surface by the saltating sand grains that releases the fine particles (dust) whose uplift by turbulence constitutes the emission flux. Therefore, saltation appears as the driving force of dust emission and it is of crucial importance to quantify its kinetic energy to relate it with the characteristics of the vertical mass flux (see below). Following Gillette and Stockton (1986), this kinetic energy is often considered to be proportional to the horizontal mass flux ( $Q$ ) in the saltation layer (Alfaro & Gomes, 2001; Alfaro et al., 1997). The fact that  $Q$  is a measure of the mass of the moving particles and increases with wind speed -as does the kinetic energy- is in favor of this assumption. In addition, via its dependence to the threshold of erosion, the magnitude of  $Q$  includes a dependence to characteristics of the surface such as soil aggregates size, presence of non-erodible elements,

crusts, or humidity, which all affect the efficiency of the entrainment. In summary,  $Q$  appears as a much better proxy of the saltation energy than wind speed alone.

Because it allows quantifying directly the dust emission mass flux ( $F_{m,v}$ ) from an estimate of the saltation flux ( $Q$ ), the so-called sandblasting efficiency ( $\alpha$ , in  $\text{m}^{-1}$ ) defined as the ratio of  $F_{m,v}$  to  $Q$  (Gillette, 1997) is of paramount importance in the modeling of the emission phase of the dust cycle. For lack of a thorough understanding of the factors controlling sandblasting, this parameter was often considered as depending only on the clay content of the emitting soil (Marticorena & Bergametti, 1995), which is to say as being independent of the aerodynamic conditions prevailing during the emission. In other words, for a given source the vertical mass flux would be simply proportional to  $Q$ . Conversely, one implication of the Dust Production Model proposed by Alfaro and Gomes (2001) is that  $\alpha$  should be negatively correlated to the kinetic energy of the saltating sand grains. Indeed, as this energy increases, an increasing fraction of it is used to release light-weight particles that do not contribute as efficiently to the vertical mass flux as the coarse ones. This means that  $\alpha$  is expected to decrease with  $Q$ , the size of the saltators, and wind speed. These extrapolations of the theory based on wind-tunnel observations were supported by a comparison with the data of the literature (Alfaro et al., 2004), but these data were sparse and more extensive studies were clearly needed to confirm this point. Now, the synchronicity of the vertical and saltation mass fluxes determinations during WIND-O-V and JADE offers the possibility to document better the factors controlling the variability of their ratio, that is, of  $\alpha$ .

Therefore, the objective of this work is to explore in depth and understand the links between the intensity of saltation, sandblasting efficiency, aerodynamic conditions (wind speed, stability of the SBL), and size distribution of the vertical dust flux. This will be achieved by making the best of the extensive experimental data collected during JADE and WIND-O-V. Note that AMMA is not included because  $Q$  was not quantified in this experiment. Section 2 (Material and Methods) recalls the characteristics of the eroding fields upon which the experiments were carried out, and briefly describes how the data were acquired and how they were used to compute the vertical dust flux by the gradient method. Section 3 (Results and comments) analyses in detail the variability of the characteristics of the saltation flux, and how these characteristics control the intensity and size distribution of the vertical dust flux. Finally, the results of this study are summarized and their implications discussed in Section 4.

## 2. Materials and Methods

The JADE Intensive Observing Period (IOP) was performed from 23 February to 13 March 2006 in a fallow wheat field cultivated the previous year, in north-west Victoria (Australia) (Ishizuka et al., 2008). The first WIND-O-V field campaign (hereinafter referred to as “WIND-O-V 2017”) took place from 1 March to 15 May 2017 in the Dar Dhaoui experimental range of the Institut des Régions Arides (IRA) of Médenine in south Tunisia (Dupont et al., 2018), whose loose sandy surface was maintained bare throughout the experiment. In spring 2018, a second campaign (WIND-O-V 2018) was carried out on the same field and with the same instrumental set-up, but in presence of sparse (3% coverage) regularly distributed vegetation. Detailed information on the methods applied during JADE can be found in Shao et al. (2011) and Ishizuka et al. (2014). For WIND-O-V-2017, we refer the reader to Khalfallah et al. (2020). In the following, we will summarize the points relevant to the present study and provide additional information on the quantification of saltation and vertical dust mass flux during the two WIND-O-V campaigns.

### 2.1. Characteristics of the Fields' Surfaces

The soils of both the Australian and Tunisian experimental fields are of the sandy type. However, the minimally-dispersed size distribution of their loose, and therefore wind-erodible, soil aggregates differ (Figure 1). The Tunisian sand grains belong mostly (96%) to a fine mode centered on approximately 90  $\mu\text{m}$  (Khalfallah et al., 2020). The remaining 4% belong to a coarse mode centered on 880  $\mu\text{m}$ . Being a mixture of particle modes centered on 70, 160, and 500  $\mu\text{m}$ , the distribution of the Australian soil is more complex.

Another difference between the two experimental sites is that the surface was regularly smoothed to favor erodibility during WIND-O-V (2017 and 2018) whereas it was not artificially altered during JADE. The consequence of this is that the threshold of erosion was quite low ( $u_{*t} = 0.22 \text{ m s}^{-1}$ ) and fairly constant over the bare field of WIND-O-V 2017 (Dupont et al., 2018), and larger and more variable (0.28–0.35  $\text{m s}^{-1}$ ) during JADE (Shao et al., 2020). As expected, the presence of sparse vegetation during WIND-O-V 2018 resulted in an increase of

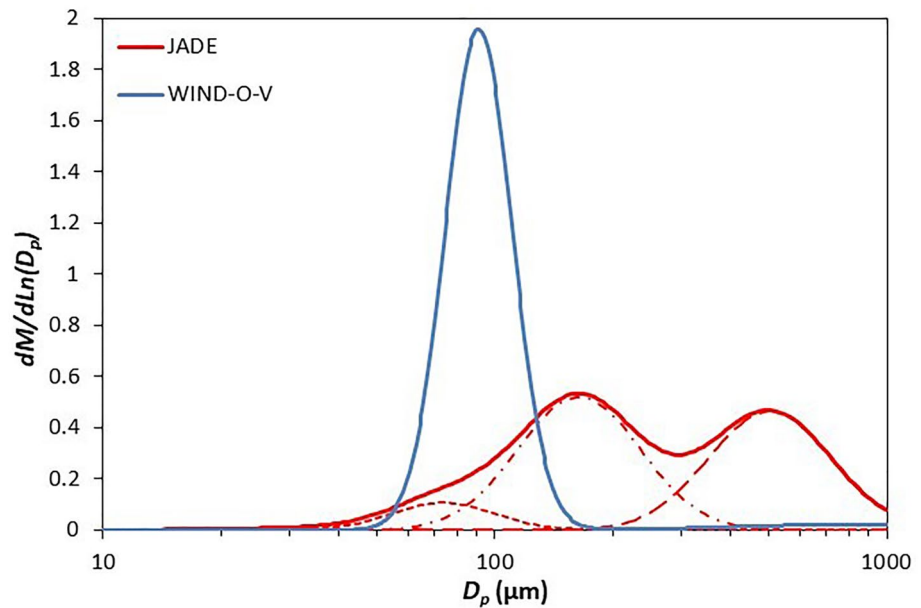


**Figure 1.** Size distribution of the sand-sized grains present at the surface of the Australian (Japanese Australian Dust Experiment [JADE]—red line) and Tunisian (WIND-O-V—blue line) experimental sites. The red dash lines correspond to the 3 particle modes of the Australian soil.

the erosion threshold ( $u_{st}$ ) that depended on the respective directions of the wind and vegetation alignments (work in preparation).

## 2.2. Measurements

### 2.2.1. Saltation Flux

During the WIND-O-V campaigns, five sand traps, the design of which was adapted from the Big Spring Number Eight (BSNE) of Fryrear (1986), were deployed in the field (Photo S2 in Supporting Information S1). Each sand trap had an opening of  $5 \times 10 \text{ cm}^2$ . They were mounted on a mast with their centers positioned at 5.5, 20.25, 36.45, 51.20, and 87.25 cm above the ground level (agl). The mast was equipped with a large wind vane so that the opening of all sand traps always faced the wind (Figure 2). They collected the moving soil grains during wind erosion periods (10 in 2017, and 6 in 2018) whose characteristics are reported in Table 1. After accounting for the collection efficiency of the sand traps (see Text S1 in Supporting Information S1 for details),  $Q$  was obtained by vertical integration of the cumulative masses collected at the 5 heights using the exponential formula proposed by Williams (1964). Thus, the WIND-O-V saltation fluxes are averages measured over durations ranging from 30 min to 3 hr and 45 min.

In JADE, 3 Sand Particle Counters (SPCs) (Mikami, Yamada, et al., 2005; Yamada et al., 2002) manufactured by Niigata Electric Co., Ltd. in Niigata, Japan) positioned at 0.1, 0.2, 0.3 m agl before day 68, then at 0.05, 0.1, and 0.3 m agl were used to measure continuously the sand fluxes in 32 size bins between 39 and  $654 \mu\text{m}$ . The horizontal fluxes and associated size distributions obtained by this method are 1 min averages of the measurements performed at the sampling rate of 1 Hz. In this work, the analysis of the temporal series of  $Q$  will be used to locate the erosion periods of the JADE campaign. Practically, the examination of the 1 min- $Q$  data shows that the

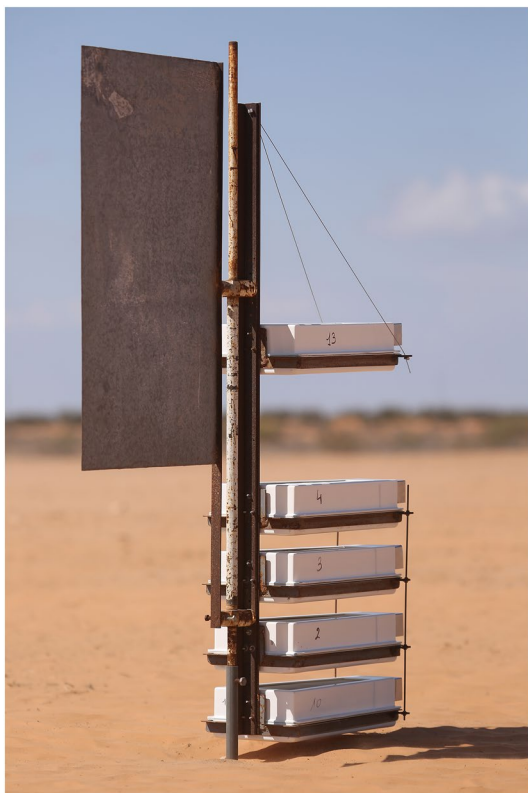


**Figure 2.** Photograph of one of the arrays of sand traps used to measure the saltation flux during WIND-O-V [©IRD-IRA, Christian Lamontagne].

**Table 1**

Characteristics of the WIND-O-V Periods (10 in 2017, and 6 in 2018) During Which the Saltation Was Measured: Year and Day of the Year (Doy), Start and End Hours (UT), 16-min Average  $u_*$  (in  $m\ s^{-1}$ ), Stability Parameter ( $z/L$ , With  $L$  the Monin Obukhov Length), Saltation Flux ( $Q$  in  $g\ m^{-1}\ s^{-1}$ ), and Sandblasting Efficiency ( $\alpha$  in  $m^{-1}$ )

Year/doy	Begin	End	$u_*$ ( $m\ s^{-1}$ )	$z/L$	$Q$ ( $g\ m^{-1}\ s^{-1}$ )	$\alpha$ ( $m^{-1}$ )
2017/66	2:45 p.m.	3:30 p.m.	0.30	-0.0201	0.26	1.57E-03
2017/67	12:15 p.m.	12:45 p.m.	0.48	-0.0085	2.96	1.10E-03
2017/68	12:00 p.m.	1:00 p.m.	0.43	-0.0166	1.83	6.83E-04
2017/68	1:45 p.m.	3:30 p.m.	0.36	-0.0174	0.40	1.09E-03
2017/74	9:00 a.m.	10:30 a.m.	0.42	-0.0076	2.66	2.30E-04
2017/74	11:30 a.m.	1:15 p.m.	0.45	-0.0086	4.25	3.26E-04
2017/110	9:15 a.m.	10:00 a.m.	0.32	-0.0331	0.48	9.10E-04
2017/110	12:15 p.m.	1:00 p.m.	0.37	-0.0307	1.20	2.74E-04
2017/110	2:15 p.m.	4:00 p.m.	0.36	-0.0143	0.93	4.47E-04
2017/122	11:30 a.m.	3:15 p.m.	0.28	-0.0706	0.19	6.45E-04
2018/94	1:42 p.m.	3:27 p.m.	0.50	-0.055	0.28	
2018/101	11:42 a.m.	12:57 p.m.	0.40	-0.047	0.64	
2018/107	1:56 p.m.	2:26 p.m.	0.62	-0.022	2.62	
2018/122	12:55 p.m.	1:40 p.m.	0.58	-0.040	1.03	
2018/122	2:25 p.m.	3:25 p.m.	0.53	-0.021	1.58	
2018/122	4:25 p.m.	5:55 p.m.	0.47	0.014	0.62	

values above approximately  $0.1\ g\ m^{-1}\ s^{-1}$  emerge from the measurement noise (Figure S1 in Supporting Information S1). For safety, we selected arbitrarily  $0.5\ g\ m^{-1}\ s^{-1}$  as the threshold above which there was no doubt that erosion was taking place. During these erosion periods, the sand grains belonging to the first 5 bins of the counters, which is to say those with diameters smaller than  $117\ \mu m$ , will be hereinafter referred to as “fine” sand as opposed to the “coarse” grains having diameters  $>117\ \mu m$  (Mikami, Yamada, et al., 2005).

### 2.2.2. Size-Resolved Vertical Mass Flux

During the intensive in-situ campaigns of JADE and WIND-O-V 2017, the size-resolved dust number concentrations were measured continuously with Optical Particle Counters (OPCs) positioned at different elevations above the eroding surface (OPC data were also acquired during WIND-O-V 2018, but due to instrumental problems, they cannot be exploited to compute the dust flux). The wind speed and air temperature vertical profiles were recorded simultaneously for the determination of the wind friction velocity and for characterizing the stability of the SBL. All these quantities are necessary for the application of the gradient method in each of the OPCs size-classes (subscript  $i$ ), and the determination of the corresponding vertical number flux ( $F_{v,i}$ ):

$$F_{v,i} = ku_* \frac{C_{l,i} - C_{h,i}}{\ln\left(\frac{z_h}{z_l}\right) - \psi_m\left(\frac{z_h}{L}\right) + \psi_m\left(\frac{z_l}{L}\right)} \quad (1)$$

In this expression,  $k$  is von Karman's constant ( $=0.4$ ),  $u_*$  is the wind friction velocity (in  $m\ s^{-1}$ ), and  $z$  the height agl (in m). The subscripts  $l$  (low) and  $h$  (high) refer to the two heights agl of the concentration ( $C$ ) measurements. The momentum stability functions ( $\psi_m$ ; e.g., Businger et al., 1971) of the dimensionless height ( $z/L$ , with  $L$  being the Monin-Obukhov length) are used to account for the instability of the SBL.

Equation 1 can be used with either mass or number concentrations and has been used to quantify the vertical dust flux in major field campaigns (Gomes et al., 2003; Khalfallah et al., 2020; Sow et al., 2009). It is still considered as a reference although it suffers from recognized limitations of different importance. For instance, Equation 1 does not properly account for the effect of SBL instability, which was shown to have an influence on the size distributions of the dust concentrations (Shao et al., 2020) and of the vertical dust flux (Khalfallah et al., 2020). A second concern is that Dupont (2020) showed that the underlying assumption of the gradient method applied

to dust, namely that turbulent transport of particles was similar to that of momentum (Gillette et al., 1972), could be challenged because of the intermittency of the dust production compared to the more continuous absorption of momentum by the surface. Regarding this last consideration, a reassuring point for the gradient method is that, when comparing it with eddy-correlation measurements, Dupont et al. (2021) showed that both methods lead overall to similar dust fluxes, at least in the small and medium size classes (i.e., between 0.37 and 3.65  $\mu\text{m}$ ) to which the eddy-covariance methods applies.

During JADE, the dust number concentrations were measured every minute in 8 size bins (0.3–0.5, 0.5–0.7, 0.7–1, 1–2, 2–3, 3–5, 5–7, and  $>7$   $\mu\text{m}$  in diameter) using three identical OPCs (Mikami, Aoki, et al., 2005; manufactured by YGK Corporation in Yamanashi, Japan) placed at heights of 1.0, 2.0, and 3.5 m agl. The wind speed and air temperature profiles were measured every minute on the same mast at two heights: at 0.50 and 2.16 m agl with cup anemometers (014A, Met One Instruments, Inc., Grants Pass, OR, USA) for wind speed, and at 1.015 and 2.813 m agl using HMP45D probes (Vaisala Corp., Vantaa, Finland) for air temperature. Though variable, the wind erosion threshold was estimated to be around 0.30  $\text{m s}^{-1}$  and  $u_*$  remained smaller than 0.60  $\text{m s}^{-1}$ . The stability of the SBL is quantified by the means of the  $z/L$  ratio. Noteworthy,  $z/L$  compares the production of turbulence by thermal instability (quantified by the vertical thermal gradient,  $\theta_*$ ) to that by wind shear (quantified by  $u_*$ ). It is negative in thermally unstable conditions, and its numerical value increases (tends toward 0) as  $u_*$  increases.

In this study, we use the results of all the erosion periods identified on the basis of the  $Q$  temporal variations. The vertical upward number dust flux is quantified first by application of Equation 1 to the number concentrations measured at 1 and 3.5 m above the field's surface. Note that the vertical flux is corrected for the effect of sedimentation and that the smallest size-class (0.3–0.5  $\mu\text{m}$ ) is not considered because its concentrations are erratic (Shao et al., 2020). In a second step, the number fluxes are converted into mass fluxes by assuming that the particles are spherical and that their mass density is that of quartz (2.65  $\text{g cm}^{-3}$ ). Finally, these mass fluxes are simply divided by the saltation flux ( $Q$ ) to obtain the sandblasting efficiency ( $\alpha$ ) at the 1' temporal resolution.

During WIND-O-V, the dust number concentrations were measured every minute in 15 size classes of equal logarithmic width ( $\text{dlog}(D) = 0.125$ ) ranging from 0.237 to 17.78  $\mu\text{m}$  using two identical OPCs (welas<sup>®</sup>, White Light Spectrometer 2300, PALAS), each equipped with an omnidirectional total suspended particles (TSP) sampling head (BGI by Mesa Labs, Butler, NJ USA) installed at 2.04 and 4.10 m agl. Wind speed and air temperature vertical profiles were determined using respectively 7 cup anemometers (A100R Vector Instrument<sup>®</sup>) positioned at 0.22, 0.65, 1.33, 1.83, 3.01, 4.00, and 5.24 m agl, and 4 thermocouples (type T copper/Constantan) positioned at 0.48, 1.66, 3.83, and 5.07 m agl on the same mast.

In all, 8 erosion events lasting from 5.4 to 9.8 hr were documented in 2017 (Khalfallah et al., 2020). After application of a rigorous quality-check, 3 135 values of the concentrations, vertical dust flux, and corresponding  $u_*$  averaged over 16 min were available for the 11 size-classes of the OPC between 0.49 and 8.66  $\mu\text{m}$ . The maximal value achieved by  $u_*$  during the campaign was 0.51  $\text{m s}^{-1}$ . As in JADE, the  $z/L$  ratio is used to characterize the stability of the SBL. Finally, the sandblasting efficiency was calculated by integrating the vertical dust flux converted into mass over the duration of the saltation measurements periods and dividing it by the corresponding  $Q$ . Note that because of the averaging over 16 min, there is inevitably more variability "hidden" in the WIND-O-V data than in the JADE ones.

### 3. Results and Comments

#### 3.1. Saltation Intensity and Size Distribution

On the basis of the  $Q$  variations, eight erosion periods could be identified in the JADE data set. These periods (D54, D57, D60–61, D62, D63, D65, D71, and D72) are named after the day (or days) of the year (doy) of their occurrence. They have variable durations, saltation intensities, and SBL conditions of stability (Figure 3; Table 2). The longest and most intense one is D71 (note that this period was split into events 10 and 11 by Ishizuka et al., 2008, and Shao et al., 2020). It started in the morning (ca. 10 a.m., local time) of day 71 and lasted 12 hr to finish in the night from day 71–72 when a small rain started to fall. Thus, at least the beginning of event D72 occurred on a surface that had been modified (displaying a weak crust) as a result of this rain event. As a consequence, the saltation threshold (about 0.35  $\text{m s}^{-1}$ ) was slightly larger on D72 than on the other days and for similar  $u_*$  the intensity of saltation was notably smaller (Figure 4).

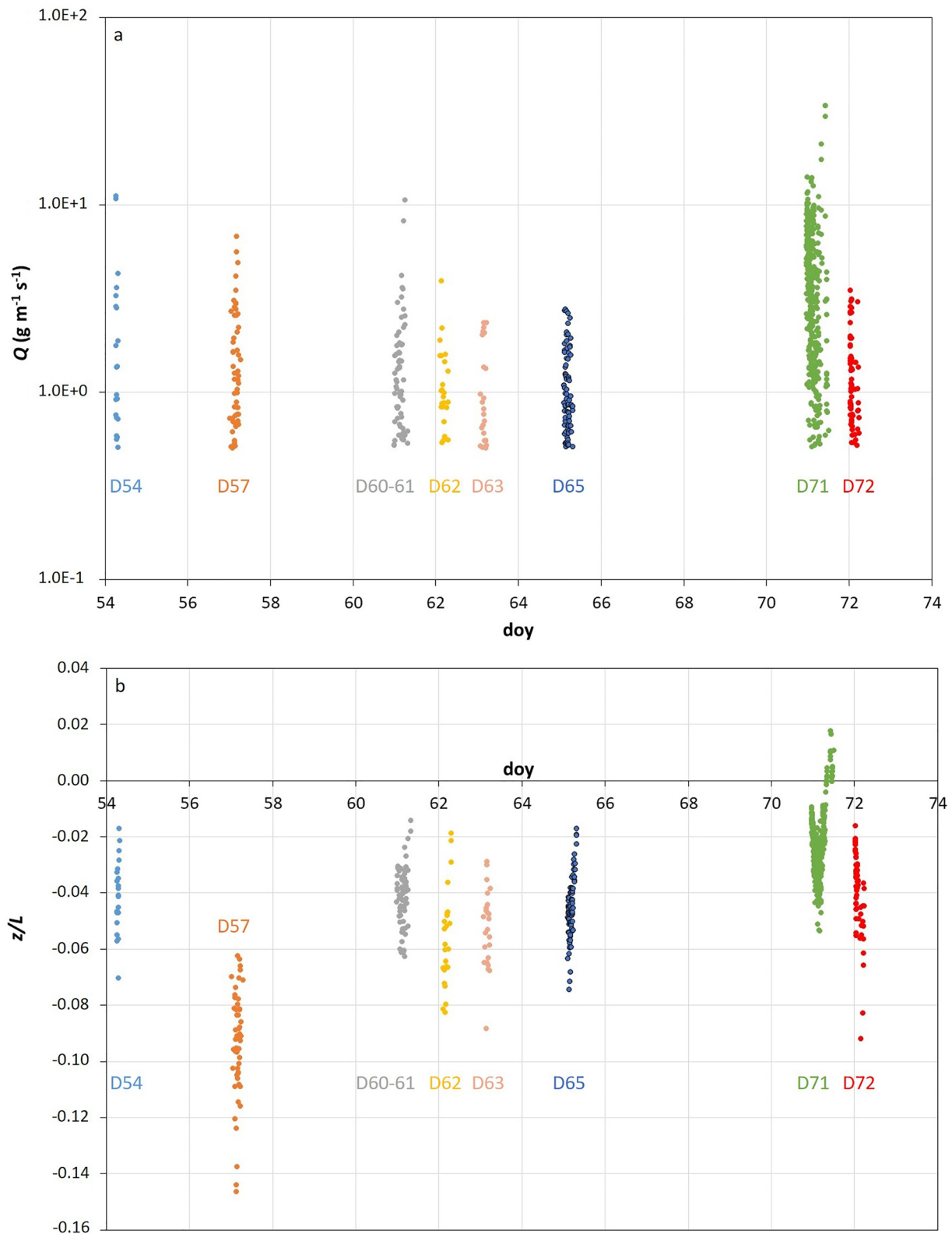


**Figure 3.** Range of variability of (a) the saltation intensity ( $Q$  in  $\text{g m}^{-1} \text{s}^{-1}$ ) and (b) stability conditions ( $z/L$ ) during the 8 events of the JADE experiments documented in this study.

**Table 2**  
Characteristics of the 8 Events of the JADE Experiments Documented in This Study: Day of the Year (Doy), Begin and Duration (Hour), Number of Available Measurements (N), 1-min Average  $u_*$  (in  $m\ s^{-1}$ ),  $z/L$ , and Saltation Flux ( $Q$  in  $g\ m^{-1}\ s^{-1}$ )

doy(s)	Begin (UT)	Duration (h)	N	$u_*$ ( $m\ s^{-1}$ )	$z/L$	$Q$ ( $g\ m^{-1}\ s^{-1}$ )
54	6:17 a.m.	1.37	21	0.37	-0.041	1.36
57	0:36 a.m.	6.38	54	0.36	-0.092	1.20
60–61	11:53 p.m.	5.17	67	0.36	-0.040	1.13
62	2:41 a.m.	4.72	24	0.31	-0.059	0.97
63	1:57 a.m.	3.78	24	0.33	-0.051	0.79
65	2:37 a.m.	4.87	80	0.35	-0.046	0.92
70–71	11:13 p.m.	13.10	352	0.39	-0.024	3.45
72	0:38 a.m.	5.22	70	0.38	-0.036	1.08

Note. Note that the local time is 11 hr ahead of the UT.

Regarding the stability conditions, they may vary significantly from one event to the other but also in the course of the longest events (Figure 3b). With an average  $z/L$  value of  $-0.092$ , D57 is by far the most unstable of the 8 events. During D71, the diurnal cycle is clearly observed with a maximal instability ( $z/L = -0.053$ ) around 2 p.m. (local time), and stable conditions ( $z/L = 0.016$ ) in the night.

For the sake of comparison, the  $Q$  measured during the WIND-O-V 2017 and WIND-O-V 2018 campaigns have also been reported in Figure 4. Despite a lower erosion threshold, the saltation fluxes measured over the bare soil of 2017 compare to those of D72, which means that they are in the lower range of the JADE values. This would need to be confirmed but a possible explanation for this rather limited intensity of the saltation flux might be the smaller size, and therefore smaller weight, of the sand grains in the Tunisian experimental plot. Interestingly, a rain event also occurred on the morning of 8 March 2017 in Dar Dhaoui. The point of the event following this rain is singled out in Figure 4 by an open black square. It can be seen that its horizontal flux is significantly below the global trend of 2017, which emphasizes again the immediate impact of modifications of the surface state and/or humidity on the erosion intensity. Similarly, the results of 2018 show that even a vegetation cover as low as 2% has a considerable effect on the saltation threshold and is able to reduce the saltation flux by more than one order of magnitude.

In summary, variations of the surface properties alter its response to the wind stress and exclude the idea of finding a simple correlation linking  $Q$  to  $u_*$ , let alone a correlation between the dust flux characteristics and  $u_*$ . The advantage of seeking how the dust flux relates to  $Q$ , via the sandblasting efficiency, rather than to  $u_*$  is to get round the variability of the surface's properties because this variability is already included in  $Q$ .

Because the range of sizes of the loose sand grains is larger in the Australian soil than in the Tunisian one, a potential dependence to aerodynamic conditions of the diameter spectrum of the wind-eroded sand grains is more likely to be observed during JADE than during WIND-O-V. In order to identify the parameters of influence, we chose to study the variability of the proportion of coarse ( $>117\ \mu m$ , as in Mikami, Yamada, et al., 2005) sand grains (%Coarse) in the saltation flux during D71. This event was selected because of its long duration and of the variability of its aerodynamic parameters. %Coarse varied between 67% and 96%, and the lowest values were recorded at the beginning and at the end of the event, which is to say in the morning and during the night. These variations are disconnected from those of  $u_*$  (Figures 5a and 5b). Conversely, %Coarse co-vary with  $z/L$  in unstable conditions (Figures 5c and 5d): sand grains coarser than  $117\ \mu m$  represent approximately 95% of  $Q$  when  $z/L < -0.04$ , and this proportion is reduced to less than 85% when tending to neutral conditions. These results are consistent with Shao et al. (2020) who already noted the influence of atmospheric stability on the size distribution of the saltation flux.

### 3.2. Sandblasting Efficiency

When  $\alpha$  is plotted against  $u_*$  or  $Q$  (Figures 6a and 6b, respectively), it becomes apparent that the sandblasting efficiency is not constant but tends to decrease as the erosion conditions become more and more energetic. This is particularly obvious for  $Q$  in Figure 6b. This general trend, observed in both JADE and WIND-O-V 2017, is consistent with the results of Alfaro et al. (2004) and thus supports indirectly the theory of Alfaro and Gomes (2001) on which this study was based. In a nutshell, the proportion of fine particles in the dust produced by sandblasting is expected to increase with  $Q$  and this replacement of coarse (heavy particles) by lighter ones reduces the mass efficiency of the sandblasting. This point will be examined further on in the following section dedicated to the size distribution of the vertical flux. However, the scatter of the experimental points around the trend is important in the two experiments. For instance, for a given saltation flux of  $1\ g\ m^{-1}\ s^{-1}$ ,  $\alpha$  varies during JADE between less than  $10^{-14}\ m^{-1}$  and more than  $10^{-13}\ m^{-1}$ . This scatter is due to differences between events

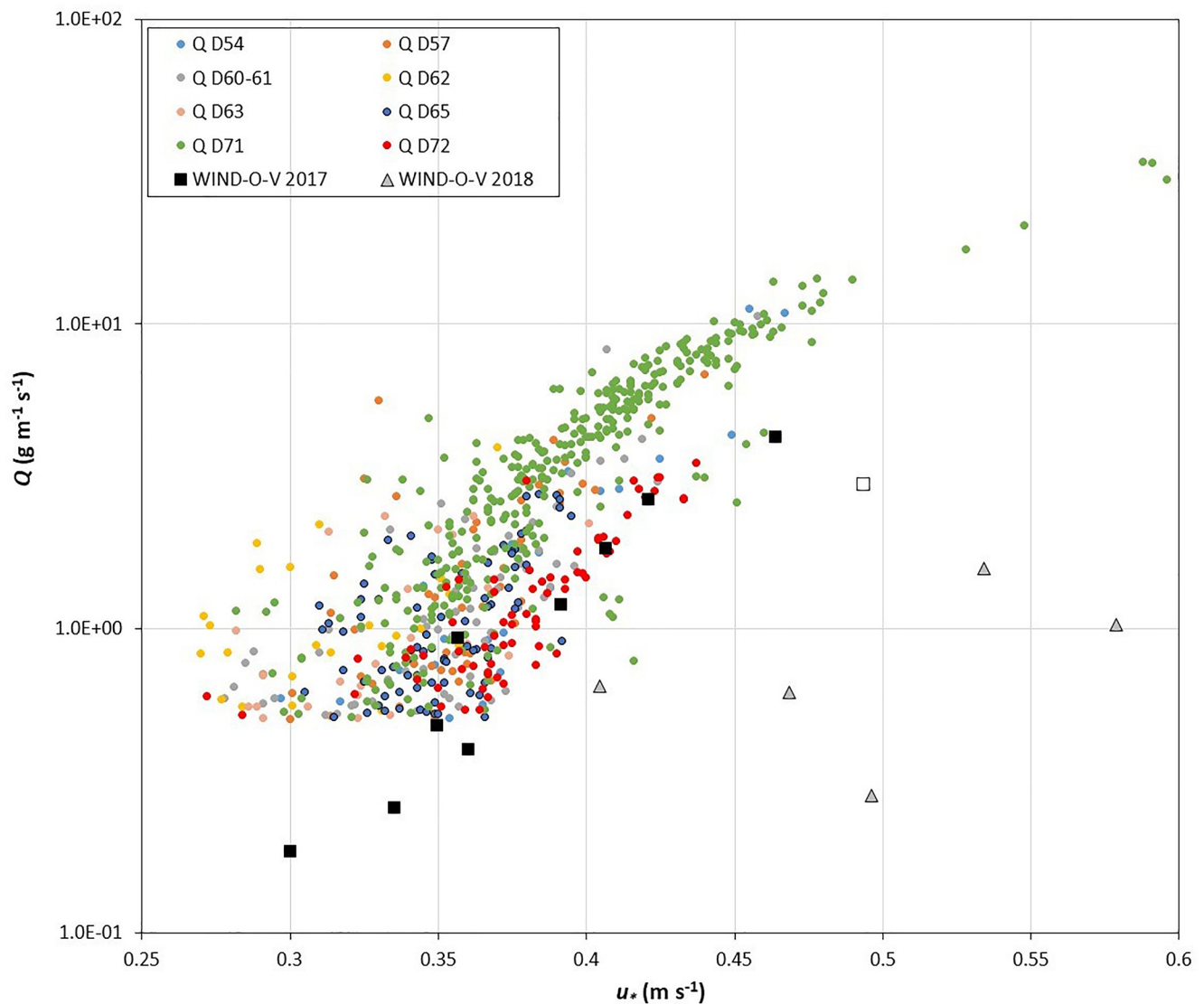


**Figure 4.** Co-variations of the saltation intensity ( $Q$  in  $\text{g m}^{-1} \text{s}^{-1}$ ) and wind friction velocity ( $u_*$  in  $\text{m s}^{-1}$ ) during the Japanese Australian Dust Experiment (JADE) (colored circles), WIND-O-V 2017 (black squares), and WIND-O-V 2018 (gray triangles) events. The black open square corresponds to the period of WIND-O-V 2017 that occurred after a rainfall. Note that the temporal resolution of the data is  $1'$  in JADE and  $16'$  in WIND-O-V.

(compare D62 and D71), but also to an important internal variability particularly obvious during some events such as D71 or D72.

Because coarse sand grains are expected to carry more kinetic energy than fine ones and to liberate finer dust, which in turn leads to lower sandblasting efficiencies, we hypothesized that at least a part of the variability of  $\alpha$  could be ascribed to the variability of the size distribution of the saltation flux. In order to test this assumption, we sorted the data of D71 in two categories according to the proportion of coarse sand grains in the horizontal flux: %Coarse-sand  $< 90\%$ , and %Coarse-sand  $> 94\%$ . The 90% and 94% limits were chosen so that each of the two horizontal flux categories contained a sufficient and similar number (82) of cases. Once this distinction is made, the results confirm (Figure 7) that the richer the horizontal flux in coarse particles, the lower the mass efficiency of the sandblasting process is. Noteworthy, an increase of just a few percent of the proportion of coarse grains in the saltation flux can reduce  $\alpha$  by up to a factor 3.

In the two categories, the decrease of  $\alpha$  with  $Q$  is well described by a power law (Figure 7). That these laws tend to converge at large  $Q$  (equivalently, at large  $u_*$ ) shows that the role played by the size of the saltators becomes

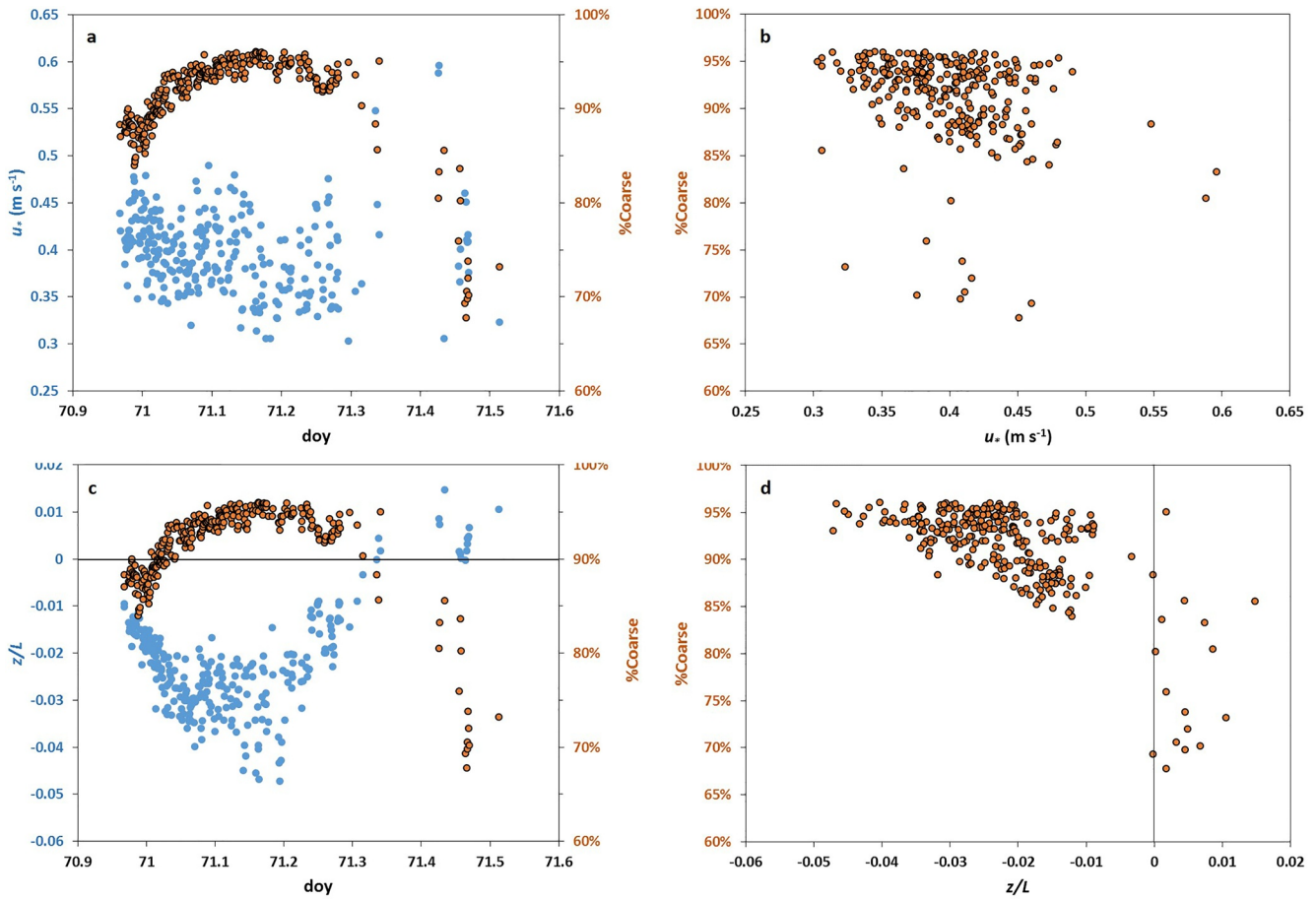


**Figure 5.** Event D71 of the Japanese Australian Dust Experiment (JADE) experiment: covariations and correlation of the proportion of coarse sand grains in the saltation flux with  $u_*$  (a and b), respectively. The color code of each plot is that indicated on the vertical axes) and  $z/L$  (c and d), respectively).

less important in very energetic conditions, most probably because the whole size-spectrum of wind-erodible sand grains is already moving and that their kinetic energy is then controlled by their speed, related to that of the wind, rather than by their mass.

In summary, the mass efficiency of the sandblasting process is not constant. It depends on the intensity of the saltation bombardment quantified by the means of  $Q$  and also, though indirectly, on the instability of the surface layer that controls the size of the saltators (Figure 5). This impact of instability is particularly important when  $Q$  is low (Figure 7), which is to say either when the characteristics of the surface (presence of non-erodible elements, crusting, humidity...) oppose the development of saltation or under moderate wind speeds. With its very low average  $Q$  ( $0.19 \text{ g m}^{-1} \text{ s}^{-1}$ ) and marked instability ( $z/L = -0.071$ ), the WIND-O-V 2017 period of day 122 (2 May) is the one that corresponds best to such criteria. This explains why its representative point appears almost as an outlier in Figure 7. Interestingly, the vertical dust flux of this day was also shown by Khalfallah et al. (2020) to be particularly rich in submicron particles. This suggests again that the sandblasting efficiency and the size distribution of the dust flux are closely linked. We will now test the validity of this assumption by studying in detail the variability of the size distribution of the vertical flux.

### 3.3. Size Distribution of the Vertical Dust Flux

In order to characterize the evolution of the size distribution of the vertical dust flux, we have calculated the proportion of fine (%fine-dust) and coarse (%Coarse-dust) dust particles in the number and mass vertical dust fluxes. Because the limits of the size classes of the OPCs used in the two experiments are not exactly the same, the “fine” dust particles are those with diameters between  $0.60$  and  $1.40 \mu\text{m}$  in JADE and between  $0.48$  and

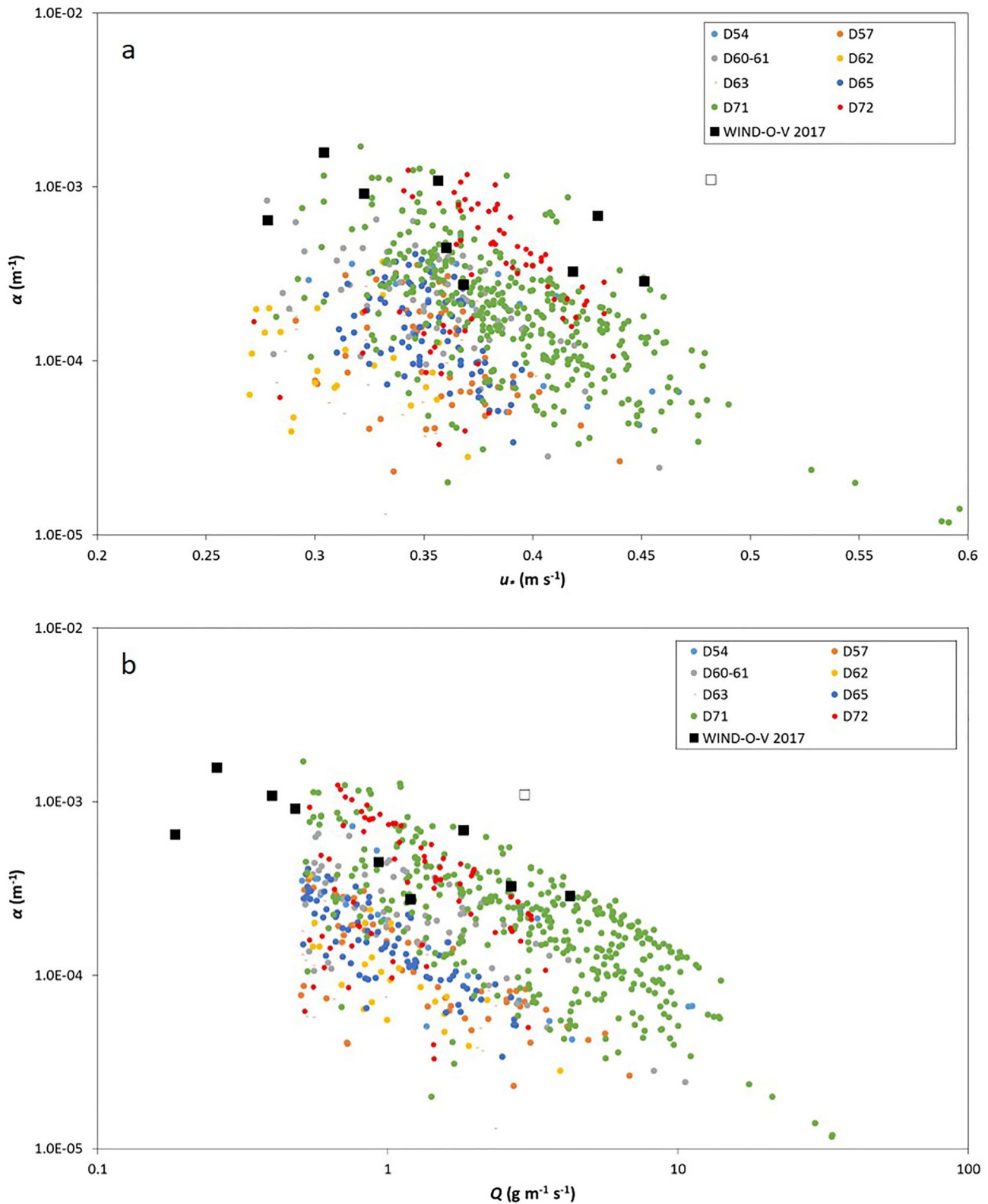


**Figure 6.** Evolution of the sandblasting efficiency ( $\alpha$  in  $\text{m}^{-1}$ ) of the Japanese Australian Dust Experiment (JADE) (colored circles; 1' temporal resolution) and WIND-O-V 2017 (black squares; 16' averages) events as a function of (a)  $u_*$  (in  $\text{m s}^{-1}$ ), and (b)  $Q$  (in  $\text{g m}^{-1} \text{s}^{-1}$ ). In WIND-O-V 2017, the black open square corresponds to the period following a rain.

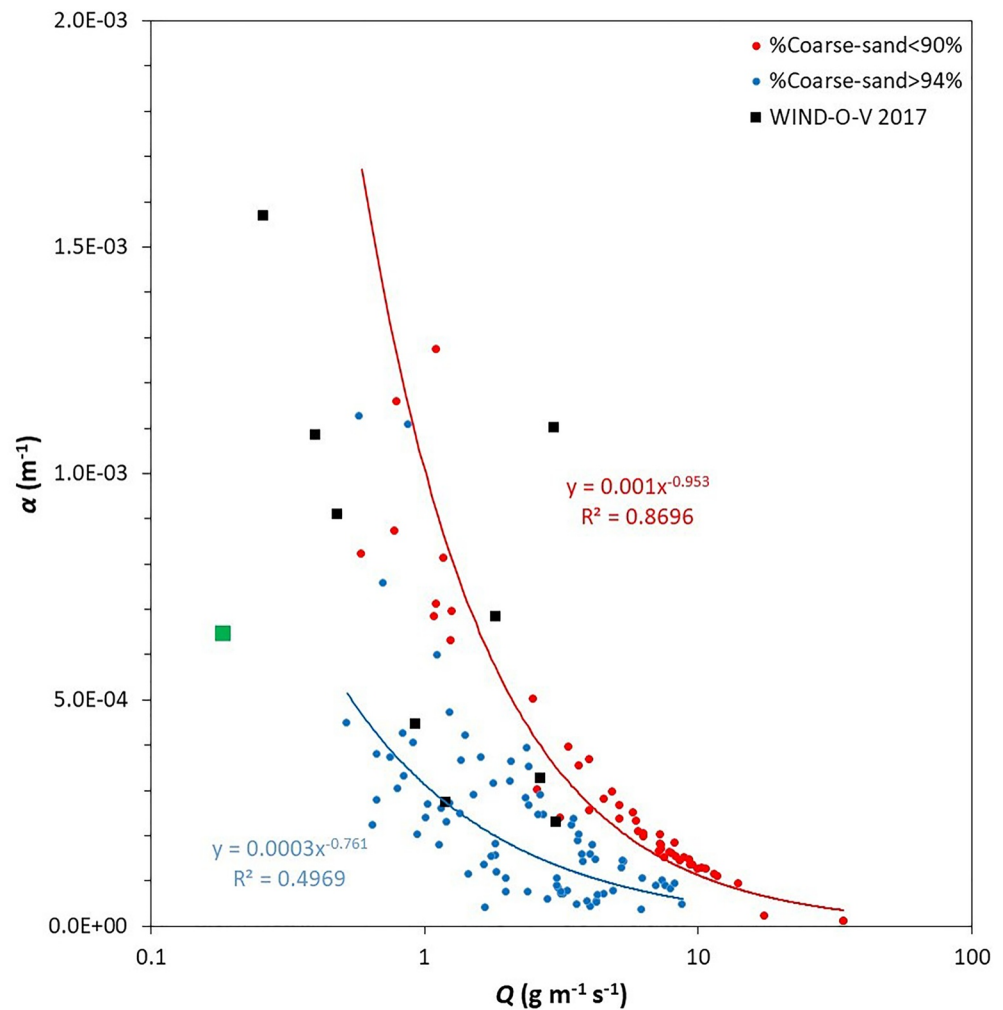


**Figure 7.** Impact of the intensity of the saltation flux ( $Q$  in  $\text{g m}^{-1} \text{s}^{-1}$ ) and its proportion of coarse sand grains (%Coarse-sand) on the efficiency of the sandblasting process ( $\alpha$  in  $\text{m}^{-1}$ ) during the longest event (D71) of the Japanese Australian Dust Experiment (JADE) experiment. The black squares correspond to the 10 WIND-O-V 2017 periods of saltation measurements except that of day 122 (2 May), which is singled out (by a green symbol) because it occurred in nearly more unstable conditions than the others.

1.15  $\mu\text{m}$  in WIND-O-V 2017. The “coarse” dust particles are those larger than 2  $\mu\text{m}$  in both cases (the upper limit being 8.39  $\mu\text{m}$  in JADE and 8.66  $\mu\text{m}$  in WIND-O-V 2017). In the following, only the variations of %coarse-dust and of the Coarse-dust/Fine-dust ratio in the number vertical dust flux will be discussed. Indeed, the proportions in the mass vertical dust flux follow exactly the same trends although the numerical values differ considerably because the mass contributed to the total vertical dust flux by the coarse dust particles overwhelms that of the fine ones (less than a few percent).

At least during some periods of JADE,  $Q$  achieved much larger values than during the WIND-O-V-2017 campaign. Therefore, the impact of  $Q$  on the size distribution is easier to observe with the JADE data (Figure 8). With values ranging from less than 20% to more than 80%, the variability of %coarse-dust is quite large at low  $Q$ . However, its range of variations narrows when  $Q$  is above approximately 5  $\text{g m}^{-1} \text{s}^{-1}$ , which occurs mostly during D71. Most of the %coarse-dust values are then between 30% and 50%. During the 10 saltation measurements periods of WIND-O-V 2017,  $Q$  was always moderate (i.e.,  $< 5 \text{ g m}^{-1} \text{ s}^{-1}$ ) and %coarse-dust varied between 20% and 50%.

The analysis of the variations of  $\alpha$  suggested that the size distribution of the vertical dust flux was sensitive to the proportion of coarse sand grains in the saltation flux. The evolution of %coarse-dust with %coarse-sand during D71 confirms this point (Figure 9): as the proportion of coarse sand grains in the saltation flux increases from

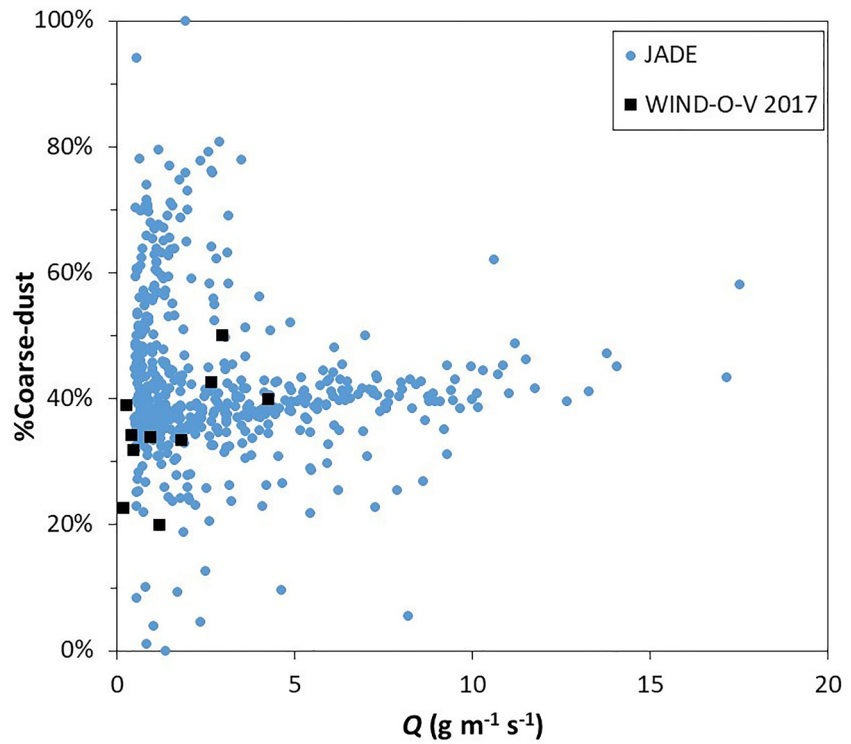


**Figure 8.** Influence of the saltation intensity ( $Q$  in  $\text{g m}^{-1} \text{s}^{-1}$ ) on the proportion of coarse particles in the vertical dust flux (%Coarse-dust) measured during D71 of Japanese Australian Dust Experiment (JADE) (blue dots) and WIND-O-V 2017 (black squares).

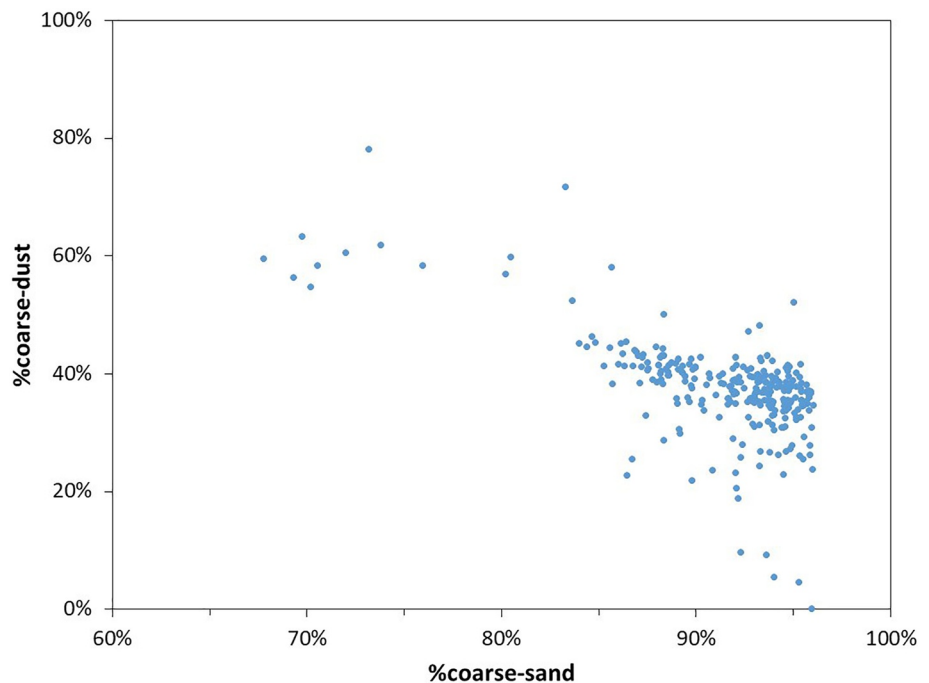


**Figure 9.** Influence of the proportion of coarse sand grains (i.e., grains with a diameter  $>117 \mu\text{m}$ ) in the saltation flux (%coarse-sand) on the proportion of dust particles coarser than  $2 \mu\text{m}$  in the vertical dust flux (%coarse-dust).

68% to 96%, the proportion of dust particles larger than 2  $\mu\text{m}$  in the vertical dust flux decreases from about 60% to 30%.

For studying the impact of the aerodynamic conditions on the relative size distribution of the vertical flux, the evolution during D71 and WIND-O-V 2017 of %coarse-dust with  $u_*$ ,  $\theta_*$  (or  $d\theta/dz$ ), and  $z/L$  are represented in Figure 10.

The proportion of coarse particles in the vertical dust flux tends to increase with  $u_*$ , which might seem contradictory with the fact that more finer particles should be emitted at large wind speed. However, in the case of D71 (Figure 10a), the overlapping of the clouds of blue and red points shows that this increase of %coarse-dust is not related to the size of the saltators. In fact, the role of  $u_*$  is complex: our interpretation of the observations is that on the one hand, large  $u_*$  tend to favor the preferential production of fine particles by sandblasting but, on the other hand, an increase in the mechanical turbulence (i.e.,  $u_*$ ) favors the vertical uplift of the particles ejected from the surface, and particularly the coarsest ones. Note that this size-dependency of the vertical uplift contradicts the assumption of Gillette et al. (1972) that the particles smaller than about 20  $\mu\text{m}$  in diameter are all equally transported by turbulence. It also means that the size distribution of the vertical dust flux measured just a few meters above an eroding surface differs from that of the dust produced by the sandblasting process: it is poorer in coarse-dust particles, and all the more so as  $u_*$  is closer to the saltation threshold.

The dependence of the %coarse-dust to thermal instability ( $\theta_*$  or  $d\theta/dz$ ) (Figures 10b and 10c) and to  $z/L$  (Figures 10d and 10e) is clearly observed. More precisely, the proportion of coarse dust particles in the vertical dust flux increases in conditions approaching neutrality. This is consistent with Shao et al. (2020) and the results detailed above showing that the size-spectrum of the sand grains set into motion by wind contained coarser grains in thermally unstable conditions than in quasi-neutral or stable ones. Therefore, all things being equal, the kinetic energy of the saltating grains increases with thermal instability and so does the proportion of fine particles produced by sandblasting.

#### 4. Summary and Conclusions

In this work, we re-analyzed the data collected essentially during the intensive measurement campaigns of the JADE and WIND-O-V 2017 experiments. Both experiments were carried out on bare sandy soils, in which there was no supply limitation of loose erodible material available for saltation and no vegetation to absorb a part of the stress exerted by the wind.

Our results show that the intensity and size distribution of the vertical dust flux over these “ideal” sandy sources are deeply connected. In the first place, they depend on the intensity of the saltation bombardment: more precisely, the larger the kinetic energy of the saltators is, the larger the proportion of fine particles released by sandblasting is and the smaller the mass efficiency of this process is. These results obtained from measurements performed in outdoor conditions are in good agreement with the predictions of the sandblasting models based on laboratory (wind-tunnel) observations. In particular, they contradict the theories considering that the PSD of the dust emitted by a bare, non-supply limited sandy surface could be independent of wind speed.

Though indirect, the role played by the stability of the SBL is also important. Our new analysis confirms the conclusions of Shao et al. (2020), namely that, at similar  $u_*$ , there are more coarse sand grains entrained in saltation in unstable conditions than under quasi-neutral stratification. Because of their important mass, these coarse grains carry more kinetic energy than the smaller ones and favor the production of fine particles. This can reduce the mass efficiency of the sandblasting process, and therefore of the intensity of the vertical dust flux, by up to a factor 3. However, these lower fluxes are particularly rich in fine particles liable to be long-range transported and whose impact on the atmospheric transfer of solar and terrestrial radiation is the largest.

In addition, contrary to the frequent assumption that all particles smaller than 20  $\mu\text{m}$  in diameter are equally uplifted by the turbulence of the SBL, our results support the findings of Khalfallah et al. (2020) by indicating that the efficiency of this uplift could be size-dependent even in the relatively narrow range of diameters (0.4–8.7  $\mu\text{m}$ ) considered in this study. Indeed, the proportion of coarse particles observed in the vertical dust flux just a few meters above the emitting surface tends to increase with  $u_*$ . In short, the role played by wind speed is dual; on the one hand, its increase favors the production of fine particles by sandblasting at the surface, but on

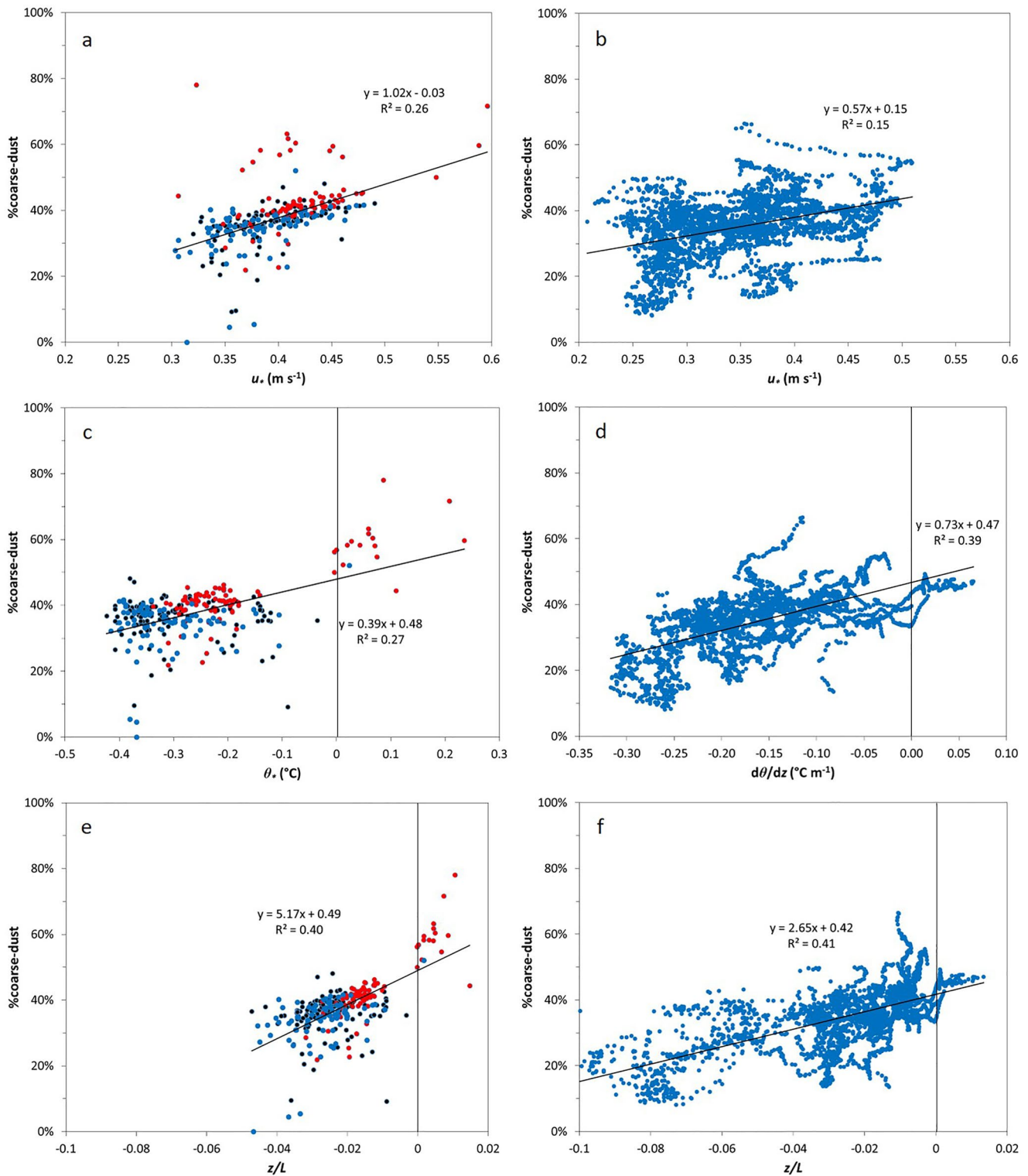


**Figure 10.** Evolution of the proportion of coarse particles in the dust flux with (a and b)  $u_*$  (in m s<sup>-1</sup>), (c and d) thermal instability (quantified by  $\theta_*$  or  $d\theta/dz$ ), and (e and f)  $z/L$  for D71 of Japanese Australian Dust Experiment (JADE) (left column) and all the WIND-O-V-2017 events (right column). For D71, the blue and red colors correspond to the two saltation categories of Figure 7. The black points are those outside them.

the other hand it facilitates the vertical entrainment of the coarse particles, which are therefore more correctly (as compared to the surface flux) represented in the vertical dust flux.

In summary, the characteristics (intensity and PSD) of the vertical dust flux measured above an eroding field are the reflect of the modulation of the dust particles produced at the surface by sandblasting by the efficiency of the vertical uplift. For instance, this vertical flux is expected to be the richest in fine dust particles when (a) the kinetic energy of the saltators is large enough to allow their production, but (b) the vertical entrainment of the coarse dust is hindered by a low degree of turbulence of the SBL. Such a conjunction of factors happens at moderate saltation intensities but under a marked thermal instability (for relatively massive grains to be entrained in saltation). This complexity, involving the influence of the SBL instability that had not been evidenced before Khalfallah et al. (2020), might explain why previous studies (e.g., Sow et al., 2009) were not able to identify any clear relationship between the size distribution of the vertical dust flux and  $u_{*c}$ .

In our reanalysis bearing essentially on measurements performed in bare conditions, the role of vegetation or modification of the surface state by rain were not really discussed beyond the limitation of  $Q$  they induced. In their recent study, Webb et al. (2021) discuss more in detail the potential importance of the presence of a sparse vegetation cover and of the supply-limitation of saltators induced by crusting on the characteristics of the emission flux. Interestingly, they conclude that in these conditions also, the emission flux tends to get richer in fine particles as wind speed increases.

Despite accumulating evidence to the contrary, many current models of the emission phase of the dust atmospheric cycle still assume that the vertical dust flux above an eroding surface is directly proportional to  $Q$ , and that its size distribution is fixed. However, the uncertainties on the characteristics of the vertical dust flux (intensity and size distribution) deriving from these simplifications are rarely estimated. Although they would probably be too complex to integrate in large-scale or even regional modeling of the dust cycle, a first important step to take in order to evaluate these uncertainties could consist in developing updated dust production models with which to perform sensitivity studies. Our results indicate that, in this development, the priority should be set on a parameterization of the saltation flux accounting for the effect of wind speed and thermal instability on its size distribution. For this, new measurements performed first in “ideal” (long fetch, non-supply limited, non-cruised, sandy fields) conditions and at high temporal resolution would be necessary to document the exact role of the aerodynamic parameters on the characteristics of the saltation flux. Once these roles are understood, a second step would consist in assessing the modifications of these characteristics induced by the presence of sparse vegetation, crusts, and limited supply of erodible material. Finally, there would be a need to understand better the physics of the size-selective vertical uptake of the fine dust particles produced by sandblasting at the soil surface.

#### Acknowledgments

The JADE project was supported by Kakenhi, Grants-in-Aid for Scientific Researches (A) from the Japan Society for the Promotion of Science (Nos. 17201008 and 20244078) and the Lower Murray-Darling Catchment Management Authority. We acknowledge the support of the French Research Agency (ANR) under the grant ANR-15-CE02-0013 (project WIND-O-V). We would like to thank: (a) Houcine Khatteli, Director of the Institut des Régions Arides (IRA) of Médenine, for the constant support of IRA in all research related to wind erosion, and in particular for giving us access to the Dar Dhaoui's experimental range and for the IRA's logistic help during the all experiment to ensure the success of the campaign, (b) the guards of the experimental stations (Noureddine Boukhli, Mokhtar Elghoul and Mousbah Elghoul) for their constant help and surveillance of the experimental system, (c) Jean Marc Bonnefond and Didier Garrigou from the Interactions Sol Plante Atmosphère laboratory (UMR INRAE 1391) for their help in the installation of the experimental device, and (d) Servanne Chevaillier, Anaïs Féron, Thierry Henry-des-Tureaux, Saâd Sekrafi, and Pascal Zapf for their contribution to the field data collection.

#### Data Availability Statement

The WIND-O-V data used in this manuscript (Rajot et al., 2022) are available for download for research and educational purposes in DataSuds at <https://doi.org/10.23708/PW2FVY>. Friction velocity and Saltation flux  $Q$  (vertically integrated saltation fluxes  $q$  at 5, 10, (20), and 30 cm heights) data set of JADE measured during from 00:16 (UT) 23 February to 23:42 13 March 2006, whose time interval is 1 min, can be downloadable from Ishizuka (2018) and from Ishizuka et al. (2021).

#### References

- Alfaro, S. C., Gaudichet, A., Gomes, L., & Maillé, M. (1997). Modeling the size distribution of a soil aerosol produced by sandblasting. *Journal of Geophysical Research*, *102*(10), 11239–11249.
- Alfaro, S. C., Gaudichet, A., Gomes, L., & Maillé, M. (1998). Mineral aerosol production by wind erosion: Aerosol particle sizes and binding energies. *Geophysical Research Letters*, *25*(7), 991–994.
- Alfaro, S. C., & Gomes, L. (2001). Modeling mineral aerosol production by wind erosion: Emission intensities and aerosol size distributions in source areas. *Journal of Geophysical Research*, *106*(D16), 18075–18084.
- Alfaro, S. C., Rajot, J. L., & Nickling, W. (2004). Estimation of PM20 emissions by wind erosion: Main sources of uncertainties. *Geomorphology*, *59*(1–4), 63–74. <https://doi.org/10.1016/j.geomorph.2003.09.006>
- Boucher, O., Randall, D., Artaxo, P., Bretherton, C., Feingold, G., Forster, P., et al. (2013). Clouds and aerosols. In T. F. Stocker, D. Qin, G.-K. Plattner, M. Tignor, S. K. Allen, J. Boschung, et al. (Eds.), *Climate change 2013: The physical basis. Contribution of working group I to the fifth assessment report of the intergovernmental panel on climate change*. Cambridge University Press.
- Businger, J. A., Wyngaard, J. C., Izumi, Y., & Bradley, E. F. (1971). Flux-profile relationships in the atmospheric surface layer. *Journal of the Atmospheric Sciences*, *28*, 181–189. [https://doi.org/10.1175/1520-0469\(1971\)028<0181:fprita>2.0.co;2](https://doi.org/10.1175/1520-0469(1971)028<0181:fprita>2.0.co;2)

- Dupont, S. (2020). Scaling of dust flux with friction velocity: Time resolution effects. *Journal of Geophysical Research: Atmospheres*, 125(1), e2019JD031192. <https://doi.org/10.1029/2019JD031192>
- Dupont, S., Rajot, J.-L., Labiadh, M., Bergametti, G., Alfaro, S. C., Bouet, C., et al. (2018). Aerodynamic parameters over an eroding bare surface: Reconciliation of the law of the wall and eddy covariance determinations. *Journal of Geophysical Research: Atmospheres*, 123(9), 4490–4508. <https://doi.org/10.1029/2017JD027984>
- Dupont, S., Rajot, J.-L., Labiadh, M., Bergametti, G., Lamaud, E., Irvine, M. R., et al. (2019). Dissimilarity between dust, heat, and momentum turbulent transports during aeolian soil erosion. *Journal of Geophysical Research: Atmospheres*, 124(2), 1064–1089. <https://doi.org/10.1029/2018JD029048>
- Dupont, S., Rajot, J.-L., Lamaud, E., Bergametti, G., Labiadh, M., Khalfallah, B., et al. (2021). Comparison between Eddy-Covariance and Flux-Gradient size-resolved dust fluxes during wind erosion events. *Journal of Geophysical Research: Atmospheres*, 126(13), e2021JD034735. <https://doi.org/10.1029/2021JD034735>
- Evan, A. T., Flamant, C., Fiedler, S., & Doherty, O. (2014). An analysis of aeolian dust in climate models. *Geophysical Research Letters*, 41(16), 5996–6001. <https://doi.org/10.1002/2014GL060545>
- Fryrear, D. W. (1986). A field dust sampler. *Journal of Soil and Water Conservation*, 41(2), 117–120.
- Gillette, D. A. (1977). Fine particle emissions due to wind erosion. *Transactions of the American Society of Agricultural Engineers*, 20, 890–897.
- Gillette, D. A., Blifford, I. H., Jr, & Fenster, C. R. (1972). Measurements of aerosol size distributions and vertical fluxes of aerosols on land subject to wind erosion. *Journal of Applied Meteorology*, 11, 977–987. [https://doi.org/10.1175/1520-0450\(1972\)011<0977:moasda>2.0.co;2](https://doi.org/10.1175/1520-0450(1972)011<0977:moasda>2.0.co;2)
- Gillette, D. A., & Stockton, P. H. (1986). Mass momentum and kinetic energy fluxes of saltating particles. In W. G. Nickling (Ed.), *Aeolian geomorphology: Binghamton geomorphology symposium 17* (1st ed., pp. 35–56). Routledge.
- Gomes, L., Rajot, J. L., Alfaro, S. C., & Gaudichet, A. (2003). Validation of a dust production model from measurements performed in semi-arid agricultural areas of Spain and Niger. *Catena*, 52(3–4), 257–271.
- Ishizuka, M. (2018). JADE data. [Dataset]. Mendeley Data. <https://doi.org/10.17632/896tx3ns6x.1>
- Ishizuka, M., Mikami, M., Leys, J., & Shao, Y. (2021). JADE data 2 (Version 1) [Dataset]. Mendeley Data. <https://doi.org/10.17632/pkvsms7ktn.1>
- Ishizuka, M., Mikami, M., Leys, J., Yamada, Y., Heidenreich, S., Shao, Y., & McTainsh, G. H. (2008). Effects of soil moisture and dried raindrop-let crust on saltation and dust emission. *Journal of Geophysical Research*, 113, D24212. <https://doi.org/10.1029/2008JD009955>
- Ishizuka, M., Mikami, M., Leys, J. F., Shao, Y., Yamada, Y., & Heidenreich, S. (2014). Power law relation between size-resolved vertical dust flux and friction velocity measured in a fallow wheat field. *Aeolian Research*, 12, 87–99. <https://doi.org/10.1016/j.aeolia.2013.11.002>
- Khalfallah, B., Bouet, C., Labiadh, M. T., Alfaro, S. C., Bergametti, G., Marticorena, B., et al. (2020). Influence of atmospheric stability on the size distribution of the vertical dust flux measured in eroding conditions over a flat bare sandy field. *Journal of Geophysical Research: Atmospheres*, 125(4), e2019JD031185. <https://doi.org/10.1029/2019JD031185>
- Klose, M., & Shao, Y. (2012). Stochastic parameterization of dust emission and application to convective atmospheric conditions. *Atmospheric Chemistry and Physics*, 12(16), 7309–7320. <https://doi.org/10.5194/acp-12-7309-2012>
- Kok, J. F. (2011a). Does the size distribution of mineral dust aerosols depend on the wind speed at emission? *Atmospheric Chemistry and Physics*, 11(19), 10149–10156. <https://doi.org/10.5194/acp-11-10149-2011>
- Kok, J. F. (2011b). A scaling theory for the size distribution of emitted dust aerosols suggests climate models underestimate the size of the global dust cycle. *Proceedings of the National Academy of Sciences*, 108(3), 1016–1021.
- Mahowald, N., Albani, S., Kok, J. F., Engelstaeder, S., Scanza, R., Ward, D. S., & Flanner, M. G. (2014). The size distribution of desert dust aerosols and its impact on the Earth system. *Aeolian Research*, 15, 53–71. <https://doi.org/10.1016/j.aeolia.2013.09.002>
- Marticorena, B., & Bergametti, G. (1995). Modeling the atmospheric dust cycle: 1. Design of a soil-derived dust emission scheme. *Journal of Geophysical Research*, 100(D8), 16415–16430.
- Middleton, N. J. (2017). Desert dust hazards: A global review. *Aeolian Research*, 24, 53–63. <https://doi.org/10.1016/j.aeolia.2016.12.001>
- Mikami, M., Aoki, T., Ishizuka, M., Yabuki, S., Yamada, Y., Gao, W., & Zeng, F. (2005). Observation of number concentration of desert aerosols in the south of the Taklimakan Desert, China. *Journal of the Meteorological Society of Japan*, 83A, 31–43. <https://doi.org/10.2151/jmsj.83A.31>
- Mikami, M., Yamada, Y., Ishizuka, M., Ishimaru, T., Gao, W., & Zeng, F. (2005). Measurement of saltation process over Gobi and sand dunes in the Taklimakan desert, China, with newly developed sand particle counter. *Journal of Geophysical Research*, 110, D18S02. <https://doi.org/10.1029/2004JD004688>
- Rajot, J. L., Bergametti, G., Labiadh, M. T., Khalfallah, B., Alfaro, S., Bouet, C., et al. (2022). Dataset of soil, saltation and gradient method measurements acquired during the WIND-O-V project in 2017 and 2018, Tunisia (Version 1) [Data set]. DataSuds. <https://doi.org/10.23708/PW2FVY>
- Shao, Y. (2001). A model for mineral dust emission. *Journal of Geophysical Research*, 106(D17), 20239–20254.
- Shao, Y., Ishizuka, M., Mikami, M., & Leys, J. F. (2011). Parameterization of size-resolved dust emission and validation with measurements. *Journal of Geophysical Research*, 116, D08203. <https://doi.org/10.1029/2010JD014527>
- Shao, Y., Raupach, M. R., & Findlater, P. A. (1993). Effect of saltation bombardment on the entrainment of dust by wind. *Journal of Geophysical Research*, 98(D7), 12719–12726. <https://doi.org/10.1029/93JD00396>
- Shao, Y., Zhang, J., Ishizuka, M., Mikami, M., Leys, J., & Huang, N. (2020). Dependency of particle size distribution at dust emission on friction velocity and atmospheric boundary-layer stability. *Atmospheric Chemistry and Physics*, 20(21), 12939–12953. <https://doi.org/10.5194/acp-20-12939-2020>
- Sow, M., Alfaro, S. C., Rajot, J. L., & Marticorena, B. (2009). Size resolved dust emission fluxes measured in Niger during 3 dust storms of the AMMA experiment. *Atmospheric Chemistry and Physics*, 9(12), 3881–3891.
- Wang, R., Li, Q., Wang, R., Chang, C., Guo, Z., Li, J., & Zhou, N. (2021). Influence of wind velocity and soil size distribution on emitted dust size distribution: A wind tunnel study. *Journal of Geophysical Research: Atmospheres*, 126(7), e2020JD033768. <https://doi.org/10.1029/2020JD033768>
- Webb, N. P., LeGrand, S. L., Cooper, B. F., Courtright, E. M., Edwards, B. L., Felt, C., et al. (2021). Size distribution of mineral dust emissions from sparsely vegetated and supply-limited dryland soils. *Journal of Geophysical Research: Atmospheres*, 126(22), e2021JD035478. <https://doi.org/10.1029/2021JD035478>
- Williams, G. (1964). Some aspects of the eolian saltation load. *Sedimentology*, 3(4), 257–287.
- Yamada, Y., Mikami, M., & Nagashima, H. (2002). Dust particle measuring system for streamwise dust flux. *Journal of Arid Land Studies*, 11(4), 229–234.
- Zhao, A., Ryder, C. L., & Wilcox, L. J. (2022). How well do the CMIP6 models simulate dust aerosols? *Atmospheric Chemistry and Physics*, 22, 2095–2119. <https://doi.org/10.5194/acp-22-2095-2022>

## References From the Supporting Information

- Ellis, J. T., Li, B., Farrell, E. J., & Sherman, D. J. (2009). Protocols for characterizing aeolian mass-flux profiles. *Aeolian Research*, *1*(1–2), 19–26. <https://doi.org/10.1016/j.aeolia.2009.02.001>
- Gillette, D. A., Fryrear, D. W., Xiao, J. B., Stockton, P., Ono, D., Helm, P. J., et al. (1997). Large-scale variability of wind erosion mass flux rates at Owens Lake 1. Vertical profiles of horizontal mass fluxes of wind-eroded particles with diameter greater than 50  $\mu\text{m}$ . *Journal of Geophysical Research*, *102*(D22), 25977–25987.
- Goossens, D., Offer, Z., & London, G. (2000). Wind tunnel and field calibration of five aeolian sand traps. *Geomorphology*, *35*(3), 233–252.
- Goossens, D., & Offer, Z. Y. (2000). Wind tunnel and field calibration of six aeolian dust samplers. *Atmospheric Environment*, *34*, 1043–1057. [https://doi.org/10.1016/s1352-2310\(99\)00376-3](https://doi.org/10.1016/s1352-2310(99)00376-3)
- Mendez, M. J., Funk, R., & Buschiazzo, D. E. (2011). Field wind erosion measurements with Big Spring Number Eight (BSNE) and Modified Wilson and Cook (MWAC) samplers. *Geomorphology*, *129*(1–2), 43–48. <https://doi.org/10.1016/j.geomorph.2011.01.011>
- Namikas, S. L. (2003). Field measurement and numerical modelling of aeolian mass flux distributions on a sandy beach. *Sedimentology*, *50*(2), 303–326.
- Panebianco, J. E., Buschiazzo, D. E., & Zobeck, T. M. (2010). Comparison of different mass transport calculation methods for wind erosion quantification purposes. *Earth Surface Processes and Landforms*, *35*(13), 1548–1555. <https://doi.org/10.1002/esp.1995>
- Shao, Y., McTainsh, G. H., Leys, J. F., & Raupach, M. R. (1993). Efficiencies of sediment samplers for wind erosion measurement. *Australian Journal of Soil Research*, *31*(4), 519–532. <https://doi.org/10.1071/SR9930519>
- Sterk, G., & Raats, P. A. C. (1996). Comparison of models describing the vertical distribution of wind-eroded sediment. *Soil Science Society of America Journal*, *60*(6), 1914–1919. <https://doi.org/10.2136/sssaj1996.03615995006000060042x>
- Wilson, S. J., & Cooke, R. U. (1980). Wind erosion. In M. J. Kirkby, & R. P. C. Morgan (Eds.), *Soil erosion*. (pp. 217–251). John Wiley & Sons.
- Zobeck, T. M., Sterk, G., Funk, R., Rajot, J. L., Stout, J. E., & Van Pelt, R. S. (2003). Measurement and data analysis methods for field-scale wind erosion studies and model validation. *Earth Surface Processes and Landforms*, *28*(11), 1163–1188. <https://doi.org/10.1002/esp.1033>